

Jet quenching and high- p_T azimuthal asymmetry ¹

I.P. Lokhtin^a, A.M. Snigirev^a and I. Vitev^b

^a Institute of Nuclear Physics, Moscow State University, 119992, Moscow, Russia

^b Iowa State University, 12 Physics Bldg. A330, Ames, IA 50011, USA

Abstract

The azimuthal anisotropy of high- p_T particle production in non-central heavy ion collisions is among the most promising observables of partonic energy loss in an azimuthally non-symmetric volume of quark-gluon plasma. We discuss the implications of nuclear geometry for the models of partonic energy loss in the context of recent RHIC data and consequences for observation of jet quenching at the LHC.

arXiv:hep-ph/0212061v1 4 Dec 2002

¹Contribution to the CERN Yellow Report on Hard Probes in Heavy Ion Collisions at the LHC.

1 Introduction

In order to interpret data on nuclear collisions from current experiments at the Relativistic Heavy Ion Collider (RHIC) and future experiments at the Large Hadron Collider (LHC), it is necessary to have knowledge of the *initial conditions*. There are large uncertainties in the estimates of the initial produced gluon density, $\rho_g(\tau_0) \sim 15 - 50/\text{fm}^3$ in central $Au + Au$ at $\sqrt{s} = 130, 200$ AGeV and $\rho_g(\tau_0) \sim 100 - 400/\text{fm}^3$ in central $Pb + Pb$ reactions at $\sqrt{s} = 5500$ AGeV, since widely different models (e.g. see [1, 2]) seem to be roughly consistent with data [3]. It is, therefore, essential to check the energy dependence of the density of the produced quark-gluon plasma (QGP) with observables complementary to the particle multiplicity dN^{ch}/dy and transverse energy dE_T/dy per unit rapidity. High- p_T observables are ideally suited for this task because they provide an estimate [4] of the energy loss, ΔE , of fast partons, resulting from medium induced non-Abelian radiation along their path, as first discussed in [5, 6] in the context of relativistic heavy ion reactions. The approximate linear dependence of ΔE on ρ_g is the key that enables high- p_T observables to convey information about the initial conditions. However, ΔE also depends non-linearly on the size, L , of the medium [7, 8] and therefore differential observables which have well controlled geometric dependences are also highly desirable.

A new way to probe ΔE in variable geometries was recently proposed in Refs. [9, 10]. The idea is to exploit the spatial azimuthal asymmetry of non-central nuclear collisions. The dependence of ΔE on the path length $L(\phi)$ naturally results in a pattern of azimuthal asymmetry of high- p_T hadrons which can be measured via the differential elliptic flow parameter (second Fourier coefficient), $v_2(p_T)$ [11, 12]. Before we show the sensitivity of the high- p_T $v_2(p_T > 2$ GeV) to different initial conditions we briefly discuss the various model calculations for the “elliptic flow” coefficient v_2 :

1. The elliptic flow parameter v_2 was first introduced in the context of *relativistic hydrodynamics* [12] and reflects the fact that due to the macroscopic sizes of large nuclei many aspects of $A + A$ collisions are driven by nuclear geometry. In non-central collisions the interaction region has a characteristic “almond-shaped” form as shown in Fig. 1.

Hydro calculations convert the ellipticity of the reaction volume into momentum space azimuthal asymmetry

$$\varepsilon = \frac{\langle x^2 \rangle - \langle y^2 \rangle}{\langle x^2 \rangle + \langle y^2 \rangle} \iff \frac{\langle p_x^2 \rangle - \langle p_y^2 \rangle}{\langle p_x^2 \rangle + \langle p_y^2 \rangle} = \langle \cos 2\phi \rangle = \frac{\int_0^{2\pi} d\phi \cos 2\phi \frac{dN^h}{dy p_T dp_T d\phi}}{\int_0^{2\pi} d\phi \frac{dN^h}{dy p_T dp_T d\phi}} \quad (1)$$

through the higher pressure gradient along the small axis. The elliptic flow is thus perfectly correlated to the reaction plane and can be used for its determination [13]. Hydrodynamic simulations [14, 15] typically describe well data from relativistic nucleus-nucleus collisions at $\sqrt{s}_{NN} = 200$ GeV up to $p_T \simeq 1.5 - 2$ GeV and it is not unlikely that at LHC energies of $\sqrt{s}_{NN} = 5.5$ TeV the region of validity of those calculations may extend to $p_T \simeq 5$ GeV.

2. Initial conditions can also be mapped onto final state observable distributions by solving covariant Boltzmann transport equations as in *cascade models* (partonic, hadronic, and multi-phase). Elliptic flow in this approach is generated via multiple elastic scatterings. Calculations are sensitive to the choice of initial conditions [16] and are currently limited by statistics to $p_T \sim 6$ GeV. It is interesting to note that they can match the high- p_T behaviour of the v_2 but require extremely large initial gluon rapidity densities $dN^g/dy \simeq 16000$ [16] and/or string melting [17].
3. Memory of the initial parton density, reaction geometry, and the consequent dynamical evolution is also retained by large transverse momentum partons (and fragmented hadrons)

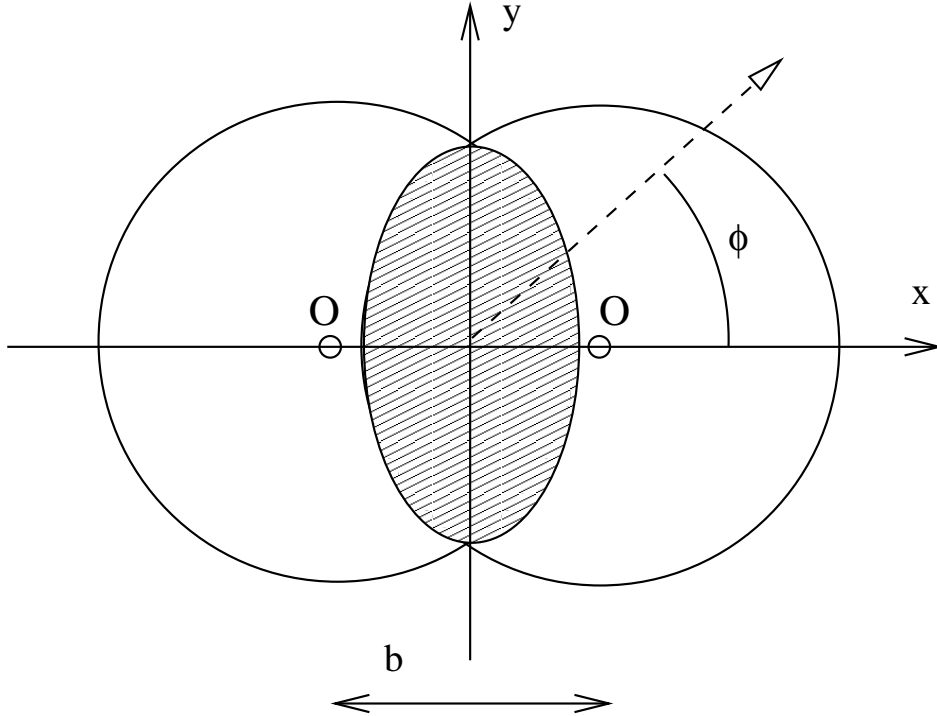


Figure 1: The nuclear overlap region in non-central $A + A$ collisions shows the importance of reaction geometry. Model calculation described here convert the spatial anisotropy illustrated above into momentum anisotropy of measured hadrons.

through their *jet quenching* pattern [9, 10]. While this approach is discussed in more detail below, it is important to emphasize here that at the single inclusive jet (or hadron) level the resulting high- p_T azimuthal asymmetry is also perfectly coupled to the reaction plane. It has been suggested that in the limit of very large energy loss the momentum asymmetry is driven by jet production from the boundary of the interaction volume [18].

4. Recently, a classical computation of the elliptic flow at transverse momenta $k_T^2 > Q_s^2$ in the framework of *gluon saturation* models has been performed [19]. It was found that the azimuthal asymmetry is generated already at proper time $\tau = 0$, i.e. it is built in the coherent initial conditions. The resulting elliptic flow coefficient was found to vanish quickly $v_2(k_T) \propto k_T^{-2}(R_x^{-2} - R_y^{-2})$ above Q_s (~ 1 GeV for RHIC and $\sim 1.4 - 2$ for LHC energies) which is not supported by the current data.
5. An approach that *does not* associate azimuthal asymmetry with the reaction plane has also been presented [20]. Both high- p_T and low- p_T v_2 emerge as a *back-to-back jet correlation bias* (with arbitrary direction relative to the reaction geometry for every p_T bin). For large transverse momenta $v_2 \propto \ln p_T/\mu$ suggest an easily detectable factor of 3 increase in going from $p_T = 5$ GeV to $p_T = 100$ GeV at LHC. The p_T -integrated $v_2 \propto 1/Q_s$ at LHC exhibits $\sim 50\%$ reduction relative to RHIC. (It can also be deduced that v_2 is larger at the SPS in comparison to RHIC in this model.)

The methods for v_2 analysis can be broadly divided in two categories: two-particle methods discussed, e.g., in [21] and multi-particle methods [22, 23]. In two-particle methods the error on the determined v_2 from non-flow (non-geometric) correlations is $\mathcal{O}(1/(v_2 M))$, where

M is the measured multiplicity. With multi-particle methods this error goes down typically to $\mathcal{O}(1/(v_2 M^2))$, i.e., smaller by a factor of order M . Although it is not possible to *completely* eliminate the non-flow components to v_2 , experimental techniques based on higher order cumulant analysis [22, 23] will be able in many cases to *clearly distinguish* between reaction geometry generated azimuthal asymmetry and back-to-back jet bias.

2 Energy loss in a longitudinally expanding plasma

We first generalize the finite energy gluon bremsstrahlung theory [8, 24, 25, 26] to take into account the expansion (neglected in [9]) of the produced gluon-dominated plasma while retaining kinematic constraints important for intermediate jet energies. The GLV reaction operator formalism [26] expands the radiative energy loss formally in powers of the mean number, χ , of interactions that the jet+gluon system suffer along their path of propagation through dense matter. For a jet produced at point \vec{x}_0 , at time τ_0 , in an *expanding* and possibly azimuthally asymmetric gluon plasma of density $\rho(\vec{x}, \tau)$, the opacity in direction $\hat{v}(\phi)$ is

$$\chi(\phi) = \int_{\tau_0}^{\infty} d\tau \sigma(\tau) \rho(\vec{x}_0 + \hat{v}(\phi)(\tau - \tau_0), \tau). \quad (2)$$

Note that the gluon-gluon elastic cross section, $\sigma(\tau) = 9\pi\alpha_s^2/2\mu_{eff}^2(\tau)$, and the density may vary along the path. The explicit closed form expression for the n^{th} order opacity expansion of the gluon radiation double differential distribution for a static medium is given in [26]. The generalization to the case of arbitrary medium similar to Eq. (2) is trivial and amounts to replacing the static weight with the nested position integrals in the case of a dynamically evolving quark-gluon plasma:

$$\frac{1}{n!} \left[\frac{L}{\lambda_g} \right]^n \implies \prod_{i=1}^n \int_0^{L-\tau_1-\dots-\tau_{i-1}} \frac{d\tau_i}{\lambda_g(\tau_i)}. \quad (3)$$

Fortunately, the opacity expansion converges very rapidly, and the first order term was found to give the dominant contribution. Higher order corrections decrease rapidly with the jet energy E . All numerical results discussed here include 2nd and 3rd order correlations between scattering centers that can alter the leading order dependence outlined analytically below.

In the case of 1+1D Bjorken longitudinal expansion with initial plasma density $\rho_0 = \rho(\tau_0)$ and formation time τ_0 , i.e.

$$\rho(\tau) = \rho_0 \left(\frac{\tau_0}{\tau} \right)^\alpha, \quad (4)$$

it is possible to obtain a closed form analytic formula [10] (under the strong *no kinematic bounds* assumption) for the energy loss due to the dominant first order term [8]. For a hard jet penetrating the quark-gluon plasma $d\Delta E^{(1)}/E dx \propto \int_{\tau_0}^{\infty} f(Z(x, \tau)) d\tau/\lambda(\tau)$, where $x \simeq \omega/E$ is the momentum fraction of the radiated gluon and the formation physics function $f(Z(x, \tau))$ is defined in [10] to be

$$f(x, \tau) = \int_0^{\infty} \frac{du}{u(1+u)} [1 - \cos(uZ(x, \tau))] . \quad (5)$$

With $Z(x, \tau) = (\tau - \tau_0)\mu^2(\tau)/2xE$ being the local formation physics parameter, two simple analytic limits of Eq. (5) can be obtained. For $x \gg x_c = \mu(\tau_0)^2 \tau_0^{\frac{2\alpha}{3}} L^{1-\frac{2\alpha}{3}}/2E = L\mu^2(L)/2E$, in which case the formation length is large compared to the size of the medium, the small $Z(x, \tau)$ limit applies leading to $f(Z) \approx \pi Z/2$. The interference pattern along the gluon path becomes important and accounts for the the non-trivial dependence of the energy loss on L .

When $x \ll x_c$, i.e. the formation length is small compared to the plasma thickness, one gets $f(Z) \approx \ln Z$. In the $x \gg x_c$ limit [10] the radiative spectrum reads:

$$\frac{d\Delta E_{x \gg x_c}^{(1)}}{dx} \approx \frac{C_R \alpha_s}{2(2-\alpha)} \frac{\mu(\tau_0)^2 \tau_0^\alpha L^{2-\alpha}}{\lambda(\tau_0)} \frac{1}{x}. \quad (6)$$

The mean energy loss (to first order in χ) is given by

$$\Delta E^{(1)} = \frac{C_R \alpha_s}{2(2-\alpha)} \frac{\mu(\tau_0)^2 \tau_0^\alpha L^{2-\alpha}}{\lambda(\tau_0)} \left(\ln \frac{2E}{\mu(\tau_0)^2 \tau_0^{\frac{2\alpha}{3}} L^{1-\frac{2\alpha}{3}}} + \dots \right). \quad (7)$$

The logarithmic enhancement with energy comes from the $x_c < x < 1$ region [26]. In the case of sufficiently large jet energies ($E \rightarrow \infty$) this term dominates. For parton energies < 20 GeV, however, corrections to this leading $\ln 1/x_c$ expression that can be exactly evaluated numerically from the GLV expression and are found to be comparable in size. The effective $\Delta E/E$ in this energy range was found to have a plateau [27]. We note that for Bjorken expansion with $\alpha = 1$, the asymptotic energy loss can be expressed in terms of the initial gluon rapidity density as

$$\Delta E_{\alpha=1}(L) \approx \frac{9C_R \pi \alpha_s^3}{4} \left(\frac{1}{\pi R^2} \frac{dN^g}{dy} \right) L \ln \frac{1}{x_c}. \quad (8)$$

It is evident from Eq. (8) that the appropriate variable to drive non-Abelian jet energy loss calculations with is the effective initial gluon rapidity density dN^g/dy .

3 Parton energy loss and nuclear geometry

For nucleus-nucleus collisions the co-moving plasma produced in an $A + B$ reaction at impact parameter b at formation time τ_0 has a transverse coordinate distribution at mid-rapidity $\rho_g(\mathbf{r}, z = 0, \tau_0)$. In studying jet production and propagation in nuclear environment it is not always technically possible to perform the Monte-Carlo averaging over the jet production points coincidentally with the simulation of parton fragmentation. It is therefore useful to separate the medium dependence of the mean jet energy loss as a function of the extent of the nuclear matter traversed and the azimuthal angle ϕ relative to the reaction plane. In the Bjorken, Eq. (4), and linear $f(Z) \approx \pi Z/2$, Eq. (5), approximations the total energy loss is proportional to a line integral along the jet trajectory $\mathbf{r}(\tau, \phi) = \mathbf{r} + \hat{v}(\phi)(\tau - \tau_0)$, averaged over the distribution of the jet production points

$$F(b, \phi) = \int d^2\mathbf{r} \frac{T_A(r) T_B(|\mathbf{r} - \mathbf{b}|)}{T_{AB}(b)} \int_{\tau_0}^{\infty} d\tau \tau \left(\frac{\tau_0}{\tau} \right)^\alpha \rho_0(\mathbf{r} + \hat{v}(\phi)(\tau - \tau_0)). \quad (9)$$

$T_A(r) = \int dz \rho_A(\mathbf{r}, z)$ and $T_{AB}(b) = \int d^2\mathbf{r} T_A(\mathbf{r}) T_B(\mathbf{r} - \mathbf{b})$ depend on the geometry. In particular, for a sharp uniform cylinder of radius R_{eff} one readily gets $T_A(r) = (A/\pi R_{\text{eff}}^2) \theta(R_{\text{eff}} - |\mathbf{r}|)$ and $T_{AB}(0) = A^2/\pi R_{\text{eff}}^2$. We can therefore define the effective radius of the sharp cylinder equivalent to a diffuse Wood-Saxon geometry via $F(0, \phi)_{\text{Wood-Saxon}} = F(0, \phi)_{\text{Sharp cylinder}}$. For $Au + Au$ collisions and $\alpha = 1$ the above constraint gives $R_{\text{eff}} \approx 6$ fm.

For a non-vanishing impact parameter b and jet direction $\hat{v}(\phi)$, we calculate the energy loss as

$$\frac{\Delta E(b, \phi)}{E} = \frac{F(b, \phi)}{F(0, \phi)} \frac{\Delta E(0)}{E} \equiv R(b, \phi) \frac{\Delta E(0)}{E}, \quad (10)$$

where the modulation function $R(b, \phi)$ captures in the *linearized* approximation the b and ϕ dependence of the jet energy loss and also provides a rough estimate of the maximum ellipticity

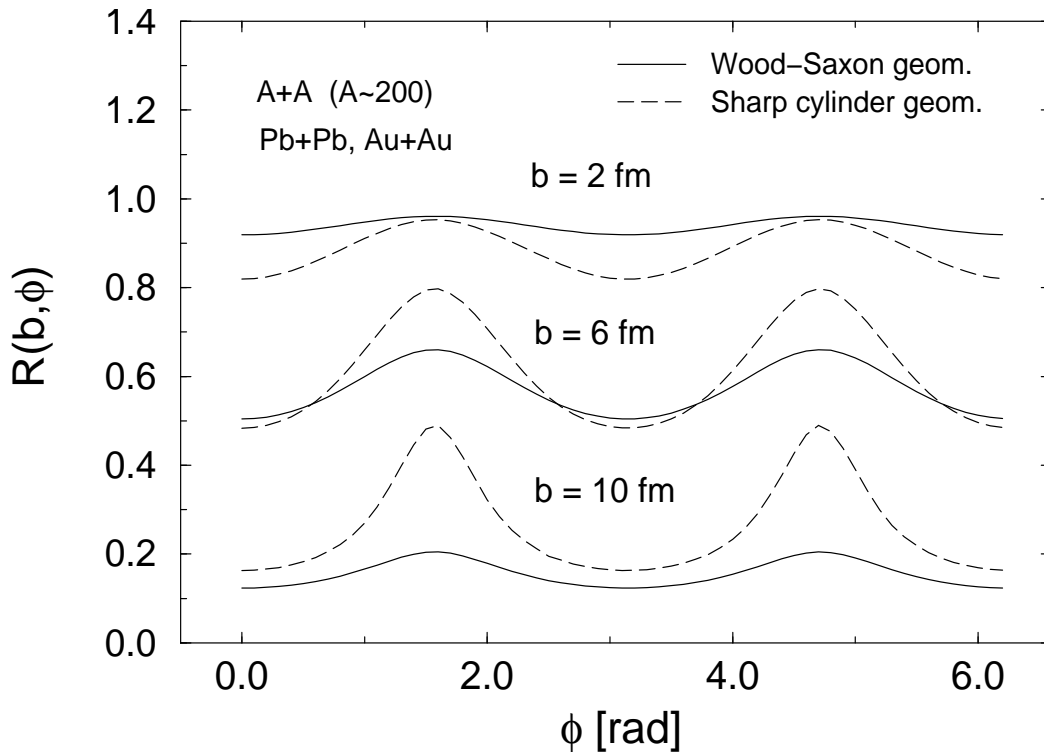


Figure 2: The modulation function $R(b, \phi)$ is plotted versus ϕ for several impact parameters $b = 2, 6, 10$ fm from Ref. [10]. Diffuse Wood-Saxon versus uniform sharp cylinder geometries are compared. The most drastic difference between these geometries occurs at high impact parameters.

generated via correlations to the reaction plane. Fig. 2 shows the $R(b, \phi)$ modulation factor plotted against the azimuthal angle ϕ for impact parameters $b = 2, 6, 10$ fm. Note that $R(b, \phi)$ reflects not only the dimensions of the characteristic “almond-shaped” cross section of the interaction volume but also the rapidly decreasing initial plasma density as a function of the impact parameter.

In order to compare to data at $p_T < 2$ GeV at RHIC and $p_T < 5$ GeV at LHC, one must also take into account the soft non-perturbative component that cannot be computed with the eikonal jet quenching formalism. The hydrodynamic elliptic flow [12] was found in [14] to have the monotonically growing form $v_{2s}(p_T) \approx \tanh(p_T/(10 \pm 2 \text{ GeV}))$ at $\sqrt{s} = 200$ AGeV and to be less sensitive to the initial conditions than the high- p_T jet quenching studied here. The interpolation between the low- p_T relativistic hydrodynamics region and the high- p_T pQCD-computable region can be evaluated as in [10].

Fig. 3 shows the predicted pattern of high- p_T anisotropy. Note the difference between sharp cylinder and diffuse Wood-Saxon geometries at $b = 7$ fm approximating roughly 20-30% central events. While the central ($b = 0$) inclusive quenching is insensitive to the density profile, non-central events clearly exhibit large sensitivity to the actual distribution. We conclude that $v_2(p_T > 2 \text{ GeV}, b)$ provides essential complementary information about the geometry and impact parameter dependence of the initial conditions in $A + A$. In particular, the rate at which the v_2 coefficient decreases at high p_T is an indicator of the diffuseness of that geometry. Minimum bias STAR data at RHIC [28, 29] for $p_T \geq 6$ GeV now seem to support the predicted [9, 10] slow decrease of v_2 at large transverse momenta. Recently in [30] hadron suppression in $Au +$

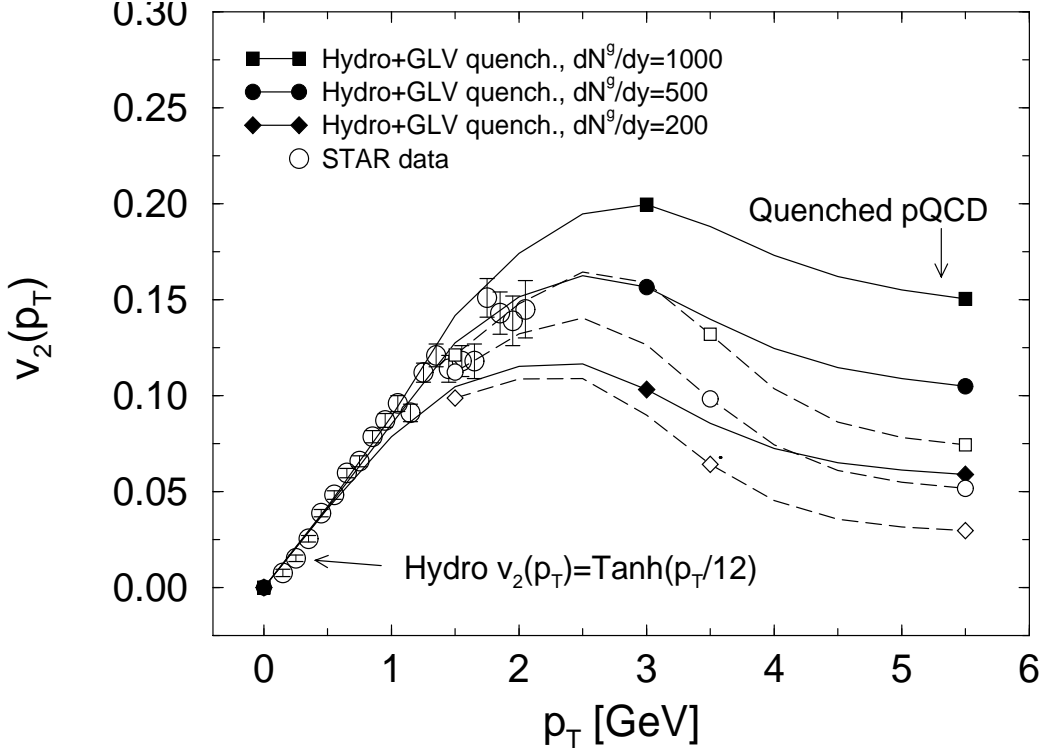


Figure 3: The interpolation of $v_2(p_T)$ between the soft hydrodynamic [14] and hard pQCD regimes is shown for $b = 7$ fm adapted from Ref. [10]. Solid (dashed) curves correspond to sharp cylindrical (diffuse Wood-Saxon) geometries presented in Fig. 2.

Au ($Pb + Pb$) relative to the binary scaled $p + p$ result at $p_T \simeq 5$ GeV for RHIC conditions ($\sqrt{s_{NN}}, dN^g/dy$) was found to be approximately equal to the quenching factor at LHC at a much larger transverse momentum scale $p_T \simeq 50$ GeV. One may thus anticipate proportionally large ($\sim 10 - 15\%$) azimuthal asymmetry for high p_T at the LHC.

4 Energy loss of jets in transversely expanding medium

Transverse expansion can only be very crudely modelled in Eq. (4) by taking $\alpha > 1$. Such approach neglects the time needed for the rarefaction wave to propagate from the surface to the center of the interaction region. To derive an improved analytic expression taking transverse flow into account, we consider next an asymmetric expanding sharp *elliptic* density profile the surface of which is defined by

$$\frac{x^2}{(R_x + v_x \tau)^2} + \frac{y^2}{(R_y + v_y \tau)^2} = 1. \quad (11)$$

The area of this elliptic transverse profile increases with time, τ , as $A_{\perp}(\tau) = \pi(R_x + v_x \tau)(R_y + v_y \tau)$. The plasma density seen by a jet in direction ϕ_0 starting from $\mathbf{x}_0 = (x_0, y_0)$ inside the ellipse with a specified initial condition $\tau_0 \rho_0 = 1/(\pi R_x R_y) dN^g/dy$ is

$$\rho(\tau, \phi_0; x_0, y_0) = \frac{1}{\pi} \frac{dN^g}{dy} \left(\frac{1}{\tau} \right) \left(\frac{1}{R_x + v_x \tau} \right) \left(\frac{1}{R_y + v_y \tau} \right)$$

$$\times \theta \left(1 - \frac{(x_0 + \tau \cos \phi_0)^2}{(R_x + v_x \tau)^2} + \frac{(y_0 + \tau \sin \phi_0)^2}{(R_y + v_y \tau)^2} \right). \quad (12)$$

We approximate the assumed ϕ_0 independent screening $\mu(\tau) \approx gT(\tau) = 2(\rho(\tau)/2)^{1/3}$ since $g \simeq 2$ and $\rho = (16\zeta(3)/\pi^2)T^3 \simeq 2T^3$ for gluon plasma and define $\tau(\phi_0)$ as the escape time to reach the expanding elliptic surface from an initial point \mathbf{x}_0 in the azimuthal direction ϕ_0 . We take $\omega(\phi_0) = 2\tau(\phi_0)(\rho(\tau(\phi_0))/2)^{2/3}$ to estimate an upper bound on the logarithmic enhancement factor. A short calculation leads to:

$$\Delta E^{(1)}(\phi_0) \approx \frac{9}{4} \frac{C_R \alpha_s^3}{R_x R_y} \frac{dN^g}{dy} \frac{\ln \frac{1+a_x \tau(\phi_0)}{1+a_y \tau(\phi_0)}}{a_x - a_y} \ln \frac{E}{\omega(\phi_0)}, \quad (13)$$

where $a_x = v_x/R_x, a_y = v_y/R_y$. This expression is a central result for transversely expanding media and provides a simple analytic generalization that interpolates between pure Bjorken 1+1D expansion for small $a_{x,y}\tau$, and 3+1D expansion at large $a_{x,y}\tau$.

In the special case of pure Bjorken (longitudinal) expansion with $v_x = v_y = 0$

$$\Delta E_{Bj}^{(1)}(\phi_0) = \frac{9C_R \alpha_s^3}{4R_x R_y} \frac{dN^g}{dy} \tau(\phi) \ln \frac{E}{\omega(\phi_0)}. \quad (14)$$

In this case, the energy loss depends *linearly* on $\tau(\phi)$ and we recover the result of Eq. (8). Another special case is azimuthally *isotropic* expansion with $R_x = R_y = R$ and $v_x = v_y = v_T$. Taking also the longitudinal Bjorken expansion into account leads in this case to

$$\Delta E_{3D}^{(1)}(\phi_0) = \frac{9}{4} \frac{C_R \alpha_s^3}{R^2} \frac{dN^g}{dy} \frac{\tau(\phi_0)}{1 + v_T \tau(\phi_0)/R} \ln \frac{E}{\omega(\phi_0)}. \quad (15)$$

We note that for a jet originating near the center of the medium and *fully penetrating* the plasma the enhanced escape time due to expansion $\tau = R/(1-v_T)$ compensates for the $1/(1+v_T \tau(\phi_0)/R)$ dilution factor. Therefore, in this isotropic case, the extra dilution due to transverse expansion has in fact no effect of the total energy loss:

$$\Delta E_{1D}^{(1)}(b = 0 \text{ fm}) \approx \Delta E_{3D}^{(1)}(b = 0 \text{ fm}), \quad (16)$$

modulo logarithmic factors which become sizable only for large v_T . An important consequence is that the inclusive azimuthally averaged jet quenching pattern in central collisions is approximately independent of transverse expansion. We have checked numerically that Eq. (16) holds for realistic transverse density profiles [14].

In non-central collisions, the azimuthal asymmetry of the mean energy loss can be expanded in a Fourier series and characterized as

$$\Delta E_{3D}^{(1)}(\phi) = \Delta E(1 + 2\delta_2(E) \cos 2\phi + \dots). \quad (17)$$

It is correlated to the final measured elliptic “flow” of jets and hadrons and has been evaluated by using a full hydrodynamic calculation from Ref. [14]. In this case we use the parameterization eBC of [14] to initialize the system and treat gluon number as conserved current to calculate the density evolution needed in the line integral Eq. (9), where it replaces the naive Bjorken $(\tau_0/\tau)^\alpha$ expansion. We average over the jet formation points the density of which is given by the number of binary collisions per unit area as in the Woods-Saxon geometry used in Ref. [10]. We find that the azimuthal asymmetry of the energy loss is strongly reduced for realistic hydrodynamic flow velocities. This implies a much smaller v_2 at high p_T than obtained in Ref. [10] where transverse expansion was not considered and poses questions about the observability of the effect at LHC.

5 LHC-specific remarks

There are several important aspects in which LHC and RHIC will differ significantly. We briefly discuss the implications of those differences for high- p_T v_2 measurements:

1. Currently at RHIC at $\sqrt{s} = 200$ AGeV the $p_T \geq 2 - 3$ GeV regime is perturbatively computable [30] (modulo uncertainties in the baryonic sector [31]). At LHC the p_T region which is not accessible through the pQCD approach may extend to transverse momenta as high as 5-10 GeV. This would imply the validity of the relativistic hydrodynamics in this domain, the extent of which can be tested by looking for marked deviations in the growth of $v_2(p_T)$, saturation, and turnover.
2. Estimates of the initial gluon rapidity density at LHC vary from $dN^g/dy = 2500$ to $dN^g/dy = 8000$. This would imply very large parton energy loss, at least in some regions of phase space. In this case jet production for moderate transverse momenta may be limited to a small shell on the surface of the interaction region, leading to a constant $v_2(p_T)$ purely determined by geometry [18].
3. Since mean transverse expansion velocities at RHIC have been estimated to be on the order of $v_T \simeq 0.5$ through relativistic hydrodynamics fits, it is natural to expect even larger values at LHC. This may lead to a significant reduction of the observed azimuthal asymmetry as discussed above. An important prediction of the approach put forth in [10] is that $v_2(p_T)$ exhibits a slow decrease with increasing transverse momentum. This can be used to distinguish azimuthal anisotropy generated through energy loss from alternative mechanisms.

5.1 Jet impact parameter dependence at the LHC

In light of the discussion in Sec. 5 it is important to assess the feasibility of azimuthal asymmetry measurements for large- E_T jets via detailed simulations. The impact parameter dependence of jet rates in $Pb + Pb$ collisions at the LHC was analyzed in [32]. The initial jet spectra at $\sqrt{s} = 5.5$ TeV were generated with PYTHIA5.7 [33]. The initial distribution of jet pairs over impact parameter b of $A + A$ collisions (without collective nuclear effects) was obtained by multiplying the corresponding nucleon-nucleon jet cross section, σ_{NN}^{jet} , by the number of binary nucleon-nucleon sub-collisions [34]:

$$\frac{d^2\sigma_{\text{jet}}^0}{d^2b}(b, \sqrt{s}) = T_{AA}(b)\sigma_{NN}^{\text{jet}}(\sqrt{s}) \left[1 - \left(1 - \frac{1}{A^2}T_{AA}(b)\sigma_{NN}^{\text{in}}(\sqrt{s}) \right)^{A^2} \right] \quad (18)$$

with the total inelastic non-diffractive nucleon-nucleon cross section $\sigma_{NN}^{\text{in}} \simeq 60$ mb.

The rescattering and energy loss of jets in a gluon-dominated plasma, created initially in the nuclear overlap zone in $Pb + Pb$ collisions at different impact parameters, were simulated. For details of this model one can refer to [32, 35]. To be specific, we treated the medium as a boost-invariant longitudinally expanding fluid according to Bjorken's solution [36] and used the initial conditions expected for central $Pb + Pb$ collisions at LHC [37, 38, 39]: formation time $\tau_0 \simeq 0.1$ fm/c, initial temperature $T_0 \simeq 1$ GeV, gluon plasma density $\rho_g \approx 1.95T^3$. For our calculations we have used the collisional part of the energy loss and the differential scattering cross section from [32]; the energy spectrum of coherent medium-induced gluon radiation was estimated using the BDMS formalism [7].

The impact parameter dependences of the initial energy density ε_0 and the averaged over φ jet escape time $\langle\tau_L\rangle$ from the dense zone are shown in Fig. 4 [32]. $\langle\tau_L\rangle$ goes down almost linearly with increasing impact parameter b . On the other hand, ε_0 is very weakly dependent

of b ($\delta\varepsilon_0/\varepsilon_0 \lesssim 10\%$) up to b on the order of nucleus radius R_A , and decreases rapidly only at $b \gtrsim R_A$. This suggests that for impact parameters $b < R_A$, where $\approx 60\%$ of jet pairs are produced, the difference in rescattering intensity and energy loss is determined mainly by the different path lengths rather than the initial energy density.

Figure 5 shows dijet rates in different impact parameter bins for $E_T^{\text{jet}} > 100$ GeV and the pseudorapidity acceptance of central part of the CMS calorimeters, $|\eta^{\text{jet}}| < 2.5$, for three cases: (i) without energy loss, (ii) with collisional loss only, (iii) with collisional and radiative loss. The total impact parameter integrated rates are normalized to the expected number of $Pb+Pb$ events during a two week LHC run, $R = 1.2 \times 10^6$ s, assuming luminosity $L = 5 \times 10^{26}$ cm $^{-2}$ s $^{-1}$. The maximum and mean values of dN^{dijet}/db distribution get shifted towards the larger b , because jet quenching is much stronger in central collisions than in peripheral ones. Since the coherent Landau-Pomeranchuk-Migdal radiation induces a strong dependence of the radiative energy loss of a jet on the angular cone size [40, 41], the corresponding result for jets with non-zero cone size θ_0 is expected to be somewhere between (iii) ($\theta_0 \rightarrow 0$) and (ii) cases. Thus the observation of a dramatic change in the b -dependence of dijet rates in heavy ion collisions as compared to what is expected from independent nucleon-nucleon reaction pattern, would indicate the existence of medium-induced parton rescattering.

Of course, such kind of measurements require the adequate determination of impact parameter in nuclear collision with high enough accuracy. It has been shown in [42] that for the CMS experiment the very forward pseudorapidity region $3 \leq |\eta| \leq 5$ can provide a measurement of impact parameter via the energy flow in the very forward (HF) CMS calorimeters with resolution $\sigma_b \sim 0.5$ fm for central and semi-central $Pb + Pb$ collisions (see details in the section on jet detection at CMS).

5.2 Jet azimuthal anisotropy at the LHC

While at RHIC the *hadron* azimuthal asymmetry at high- p_T is being analyzed, at LHC energies one can hope to observe similar effects for the hadronic jet itself [35] due to the large inclusive cross section for hard jet production on a scale $E_T \sim 100$ GeV.

The anisotropy of the energy loss (ΔE) goes up with increasing b , because the azimuthal asymmetry of the interaction volume gets stronger. However, the absolute value of the energy loss goes down with increasing b due to the reduced path length L (and ε_0 at $b \gtrsim R_A$, see Fig. 4). The non-uniform dependence of ΔE on the azimuthal angle φ is then mapped onto the jet spectra in semi-central collisions. Figure 6 from [35] shows the distribution of jets over φ for the cases with collisional and radiative loss (a) and collisional loss only (b) for $b = 0, 6$ and 10 fm. The same conditions and kinematical acceptance as in Fig. 5 were fulfilled. The distributions are normalized by the distributions of jets as a function of φ in $Pb + Pb$ collisions without energy loss. The azimuthal anisotropy becomes stronger in going from central to semi-central reactions, but the absolute suppression factor is reduced with increasing b . For jets with finite cone size one can expect the intermediate result between cases (a) and (b), because, as we have mentioned before, radiative loss dominates at relatively small angular sizes of the jet cone $\theta_0 (\rightarrow 0)$, while the relative contribution of collisional loss grows with increasing θ_0 .

In non-central collisions the jet distribution over φ is approximated well by the form $A(1 + B \cos 2\varphi)$, where $A = 0.5(N_{\text{max}} + N_{\text{min}})$ and $B = (N_{\text{max}} - N_{\text{min}})/(N_{\text{max}} + N_{\text{min}}) = 2 \langle \cos 2\varphi \rangle$. In the model [35] the coefficient of jet azimuthal anisotropy, $v_2^{\text{jet}} \equiv \langle \cos 2\varphi^{\text{jet}} \rangle_{\text{event}}$, increases almost linearly with the impact parameter b and becomes maximum at $b \sim 1.2R_A$. After that v_2^{jet} drops rapidly with increasing b : this is the domain of impact parameter values where the effect of decreasing energy loss due to the reduction of the effective transverse size of the dense zone and the initial energy density of the medium is crucial and cannot be compensated by the stronger volume ellipticity. Another important feature is that the jet azimuthal anisotropy

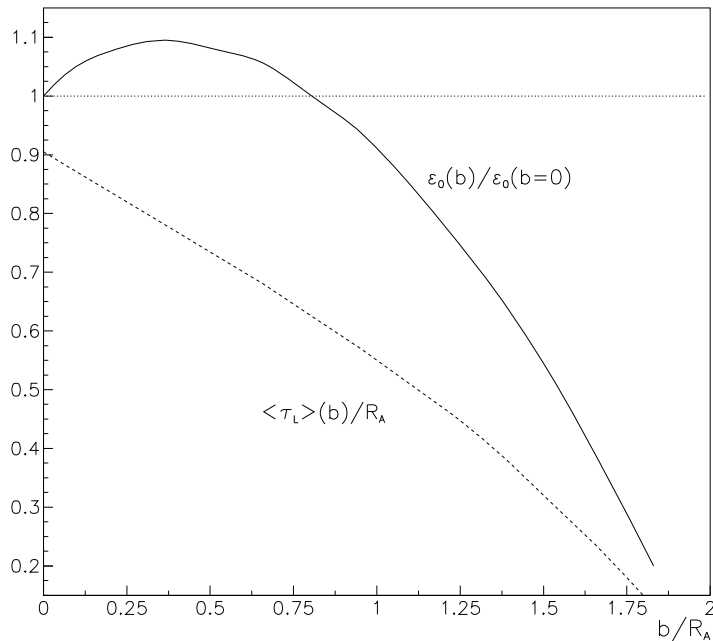


Figure 4: The impact parameter dependence of the initial energy density $\varepsilon_0(b)/\varepsilon_0(b=0)$ in nuclear overlap zone (solid curve), and the average proper jet escape time $\langle\tau_L\rangle/R_A$ of from the dense matter (dashed curve) [32].

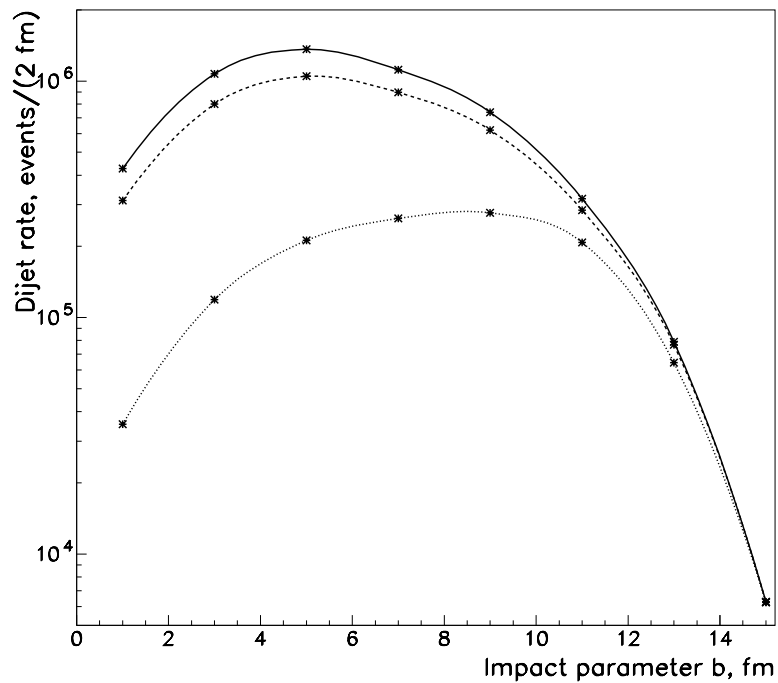


Figure 5: The jet+jet rates for $E_T^{\text{jet}} > 100$ GeV and $|\eta^{\text{jet}}| < 2.5$ in different impact parameter bins: without energy loss (solid curve), with collisional loss (dashed curve), with collisional and radiative loss (dotted curve) [32].

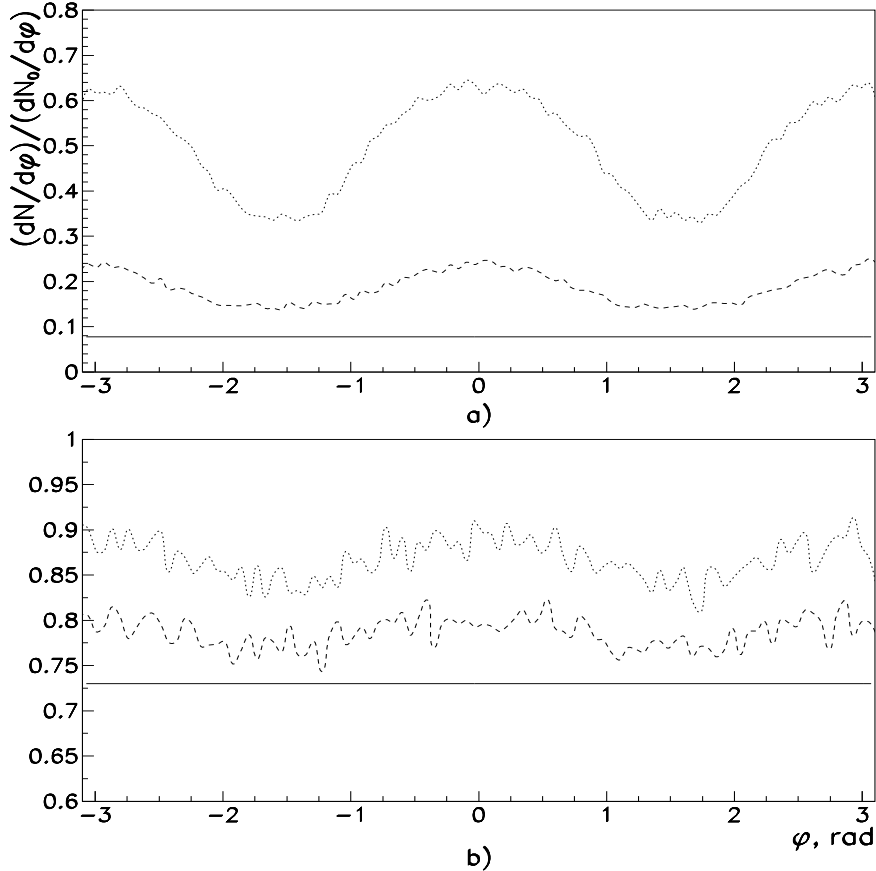


Figure 6: The jet distribution over azimuthal angle for the cases with collisional and radiative loss (a) and collisional loss only (b), $E_T^{\text{jet}} > 100$ GeV and $|\eta^{\text{jet}}| < 2.5$ [35]. The histograms (from bottom to top) correspond to the impact parameter values $b = 0, 6$ and 10 fm.

decreases with increasing jet energy, because the energy dependence of medium-induced loss is rather weak (absent in the BDMS formalism and $\sim \ln E$ in the GLV formalism for the radiative part at high E_T).

The advantage of azimuthal jet observables is that one needs to reconstruct only the direction of the jet, not its total energy. It can be done with high accuracy, while reconstruction of the jet energy is more ambiguous. However, analysis of jet production as a function of the azimuthal angle requires event-by-event measurement of the angular orientation of the reaction plane. The methods summarized in Ref. [11, 43, 44] present ways for reaction plane determination. They are applicable for studying anisotropic particle flow in current heavy ion dedicated experiments at the SPS and RHIC, and may be also used at the LHC [35]. Recently a method for measuring jet azimuthal anisotropy coefficients without event-by-event reconstruction of the reaction plane was proposed [45]. This technique is based on the correlations between the azimuthal position of jet axis and the angles of hadrons not incorporated in the jet. The method has been generalized by taking as weights the particle momenta or the energy deposition in the calorimetric sectors. It was shown that the accuracy of the method improves with increasing multiplicity and particle (energy) flow azimuthal anisotropy, and is practically independent of the absolute values of azimuthal anisotropy of the jet itself.

6 Conclusions

The azimuthal anisotropy of high- p_T hadron production in non-central heavy ion collisions is shown to provide a valuable experimental tool for studying both gluon bremsstrahlung in non-Abelian media and the properties of the reaction volume such as its size, shape, initial parton (number and energy) rapidity densities, and their subsequent dynamical evolution. The *saturation* and the *gradual decrease* at large transverse momentum of the reaction geometry generated v_2 , predicted as a signature complementary to jet quenching of strong radiative energy loss in a dense QCD plasma [10], seem now supported by preliminary data extending up to $p_T \simeq 10$ GeV at RHIC.

The initial gluon densities in $Pb + Pb$ reactions at $\sqrt{s_{NN}} = 5.5$ TeV at the Large Hadron Collider are expected to be significantly higher than at RHIC, implying even stronger partonic energy loss. This may result in interesting novel features of jet quenching, such as modification of the jet distribution over impact parameter [32] in addition to the azimuthal anisotropy of the jet spectrum. The predicted large cross section for hard jet production on a scale of $E_T \sim 100$ GeV will allow for a systematic study of the differential nuclear geometry related aspects of jet physics at the LHC.

7 Acknowledgements

The authors are grateful to J.Y. Ollitrault for helpful discussion and proof reading this manuscript. It is pleasure to thank L.I. Sarycheva and U. Wiedemann for encouraging and interest in this work. We are much indebted to K. Filimonov and P. Jacobs for comments on the STAR high- p_T v_2 data. I.V. is supported by the United States Department of Energy under Grant No. DE-FG02-87ER40371.

References

- [1] X. N. Wang and M. Gyulassy, Phys. Rev. D **44** (1991) 3501.
- [2] K. J. Eskola, K. Kajantie, P. V. Ruuskanen and K. Tuominen, Nucl. Phys. B **570** (2000) 379.
- [3] B. B. Back *et al.* [PHOBOS Collaboration], Phys. Rev. Lett. **85** (2000) 3100.
- [4] X. N. Wang and M. Gyulassy, Phys. Rev. Lett. **68** (1992) 1480.
- [5] M. Gyulassy and X. N. Wang, Nucl. Phys. B **420** (1994) 583.
- [6] X. N. Wang, M. Gyulassy and M. Plumer, Phys. Rev. D **51**, 3436 (1995).
- [7] R. Baier, Yu.L. Dokshitzer, A.H. Mueller and D. Schiff, Nucl. Phys. B **531** (1998) 403.
- [8] M. Gyulassy, P. Levai and I. Vitev, Phys. Rev. Lett. **85** (2000) 5535.
- [9] X. N. Wang, Phys. Rev. C **63** (2001) 054902.
- [10] M. Gyulassy, I. Vitev and X. N. Wang, Phys. Rev. Lett. **86** (2001) 2537.
- [11] S.A. Voloshin and Y. Zhang, Z. Phys. C **70** (1996) 665.
- [12] J. Y. Ollitrault, Phys. Rev. D **46** (1992) 229.
- [13] J. Y. Ollitrault, Phys. Rev. D **48** (1993) 1132.

- [14] P. F. Kolb, U. W. Heinz, P. Huovinen, K. J. Eskola and K. Tuominen, Nucl. Phys. A **696** (2001) 197.
- [15] D. Teaney, J. Lauret, and E.V. Shuryak, nucl-th/0110037.
- [16] D. Molnar and M. Gyulassy, Nucl. Phys. A **697** (2002) 495 [Erratum-ibid. A **703** (2002) 893].
- [17] Z. W. Lin and C. M. Ko, Phys. Rev. C **65** (2002) 034904.
- [18] E. V. Shuryak, Phys. Rev. C **66** (2002) 027902.
- [19] D. Teaney and R. Venugopalan, Phys. Lett. B **539** (2002) 53.
- [20] Y. V. Kovchegov and K. L. Tuchin, Nucl. Phys. A **708** (2002) 413.
- [21] S. Wang *et al.*, Phys. Rev. C **44** (1991) 1091.
- [22] N. Borghini, P. M. Dinh and J. Y. Ollitrault, Phys. Rev. C **64** (2001) 054901.
- [23] N. Borghini, P. M. Dinh and J. Y. Ollitrault, nucl-ex/0110016.
- [24] M. Gyulassy, P. Levai and I. Vitev, Nucl. Phys. A **661** (1999) 637
- [25] M. Gyulassy, P. Levai and I. Vitev, Nucl. Phys. B **571** (2000) 197
- [26] M. Gyulassy, P. Levai and I. Vitev, Nucl. Phys. B **594** (2001) 371.
- [27] P. Levai, G. Papp, G. Fai and M. Gyulassy, J. Phys. G **28** (2002) 2059.
- [28] K. Filimonov [STAR Collaboration], arXiv:nucl-ex/0210027.
- [29] P. Jacobs, arXiv:hep-ex/0211031.
- [30] I. Vitev and M. Gyulassy, arXiv:hep-ph/0209161, Phys. Rev. Lett. in press.
- [31] I. Vitev and M. Gyulassy, Phys. Rev. C **65** (2002) 041902.
- [32] I.P. Lokhtin and A.M. Snigirev, Eur. Phys. J. C **16** (2000) 527.
- [33] T. Sjöstrand, Comput. Phys. Commun. **82** (1994) 74.
- [34] R. Vogt, Heavy Ion Phys. **9** (1999) 339.
- [35] I.P. Lokhtin, S.V. Petrushanko, L.I. Sarycheva and A.M. Snigirev, [arXiv:hep-ph/0112180], Proceeding of International Conference on Physics and Astrophysics of Quark-Gluon Plasma (Jaipur, India, 26-30 Nov 2001); Phys. At. Nucl. **65** (2002) 943.
- [36] J.D. Bjorken, Phys. Rev. D **27** (1983) 140.
- [37] K.J. Eskola, K. Kajantie and P.V. Ruuskanen, Phys. Let. B **332** (1994) 191.
- [38] K.J. Eskola, Prog. Theor. Phys. Suppl. **129** (1997) 1.
- [39] K.J. Eskola, Comments Nucl. Part. Phys. **22** (1998) 185.
- [40] I.P. Lokhtin and A.M. Snigirev, Phys. Lett. B **163** (1998) 440.
- [41] R. Baier, Yu.L. Dokshitzer, A.H. Mueller and D. Schiff, Phys. Rev. C **58** (1998) 1706.

- [42] I. Damgov *et al.*, Part. Nucl. Lett. **107** (2001) 93; CERN CMS Note 2001/055.
- [43] J. Y. Ollitrault, arXiv:nucl-ex/9711003.
- [44] A.M. Poskanzer and S.A. Voloshin, Phys. Rev. C **58** (1998) 1671.
- [45] I.P. Lokhtin, L.I. Sarycheva and A.M. Snigirev, Phys. Lett. B **537** (2002) 261.